

# Reactive Blending Approach to Modify Spin-Coated Epoxy Film: Part I. Synthesis and Characterization of Star-Shaped Poly( $\epsilon$ -caprolactone)

Markus P. K. Turunen, Tomi Laurila, Jorma K. Kivilahti

Department of Electrical and Communications Engineering, Laboratory of Electronics Production Technology, Helsinki University of Technology, FIN-02015 HUT, Finland

Received 28 June 2004; accepted 10 June 2005

DOI 10.1002/app.22832

Published online in Wiley InterScience (www.interscience.wiley.com).

**ABSTRACT:** To effectively modify the properties of an epoxy, branched oligomers were synthesized from  $\epsilon$ -caprolactone (CL) and end-functionalized to realize network precursors that can be reactively blended with the epoxy. The ring-opening polymerization (ROP) of the CL in the presence of polyglycerol (PGL) initiator (3.9 and 9.1 mol %) and Sn(II) 2-ethylhexanoate catalyst yielded oligomers with hydroxyl end-groups, which were converted to carboxylic acid functionality by reaction with succinic anhydride. The functionalized oligomers had a four-armed structure and the molecular weight of the oligomers could be controlled by the ratio of CL to PGL in the feed. To achieve an adequately crosslinked network in the reactive blending, a dual-catalyzed reaction scheme was employed. First the oligomer was

incorporated into the epoxy matrix in an imidazole-catalyzed reaction and then the crosslinking was completed with an acid-catalyzed ROP of the residual epoxies. Investigations showed that toughened coatings could be prepared from the inherently brittle epoxy through proper choice of the blending ratio of oligomer to epoxy. The blending increased surface hydrophobicity at high concentrations of functionalized oligomer, but did not have an adverse effect on the inherently advantageous endothelial cell spreading. © 2006 Wiley Periodicals, Inc. *J Appl Polym Sci* 101: 3677–3688, 2006

**Key words:** oligomers; ring-opening polymerization; crosslinking; phase separation; modification

## INTRODUCTION

Epoxyes are extensively used in the manufacture of electronic devices because of their excellent adhesive properties, suitable mechanical and dielectric properties, light weight, and low cost. Use of photodefinable epoxyes for high aspect ratio patterning has enabled many innovative applications, including microfluidic components, lab-on-a-chip instruments, miniaturized micromotors, and scanning microprobes, besides the conventional uses of epoxyes such as coatings and films.<sup>1–9</sup> Surface modifications have provided good interfacial adhesion between polymers and metallizations,<sup>10–14</sup> allowing reliable manufacture of complex modules frequently encountered in microelectromechanical systems (MEMS)<sup>15,16</sup> and highly miniaturized electronics.<sup>17,18</sup>

The reliability of miniaturized electronics and the packaging density that is ever-increasing create strict demands on interconnections, in particular, and interfacial reliability including thermomechanical compatibility has become an important issue.<sup>1,10,19,20</sup> Re-

cently, we have studied the manufacture of integrated optical waveguides and highly miniaturized build-up modules using SU8 and other epoxyes and rigid printed wiring boards (PWBs) as substrates.<sup>10,19,21,22</sup> Today, however, flexible PWBs are increasingly being used in high-density applications such as smart cards, hearing aids, displays, and portable electronics.<sup>23</sup>

Blending of brittle epoxyes like the SU8<sup>24</sup> with a phase-separating polymer is a common approach to the toughening of epoxyes. Most of the modifiers are liquid rubbers, the carboxyl-terminated copolymer of acrylonitrile and butadiene (CTBN) being especial widely used.<sup>25,26</sup> CTBN reacts with the epoxy matrix to provide effective toughening. However, there are some serious drawbacks to CTBN. Its unsaturated double bonds offer sites for oxidative as well as thermal degradation. Moreover, traces of carcinogenic acrylonitrile may persist, preventing the use of CTBN in biomaterials.<sup>27,28</sup> Several studies have described the use of nonreactive phase-separating thermoplastic polymer modifiers.<sup>26,27,29–32</sup> Unfortunately, toughening by nonreactive blending has too often been at the expense of elastic modulus and thermal properties. In contrast to this, controlled crosslinking between the blending polymer and the brittle resin has been reported to result in a tough network without the adverse effects.<sup>33,34</sup>

Correspondence to: M. P. K. Turunen (markus.turunen@hut.fi).

In an earlier research,<sup>35,36</sup> we described the synthesis and crosslinking of star-shaped poly( $\epsilon$ -caprolactone) (PCL). Others have reported that highly branched polymers effectively flexibilize inherently brittle epoxies.<sup>37,38</sup> The objective of the present work was to find out if a star-shaped PCL could be tailor-made and functionalized to enable crosslinking with SU8 epoxy resin. With this target in mind, we synthesized four-armed CL-based oligomers and end-functionalized them with carboxylic acid groups. In this article, we describe the synthesis of the oligomers, their reactive blending with SU8 epoxy, and selected surface and bulk properties of spin-coated films. In part II,<sup>39</sup> we will report the crosslinking kinetics of the dual-catalyzed crosslinking reaction.

## METHODS

### Materials

Oligomers were synthesized from  $\epsilon$ -caprolactone monomer (CL; Solvay) in the presence of Sn(II) 2-ethylhexanoate (SnOct<sub>2</sub>; Sigma) catalyst and polyglycerol-3 (PGL; Solvay) initiator. According to the manufacturer, the PGL contained five hydroxyl groups. CL was dried over molecular sieves and the other materials were used as-received. Succinic anhydride (SA; Fluka) was used in the end-functionalization. The epoxy resin was SU8 (Shell) containing eight functional groups per monomer ( $\bar{M}_n = 7000$  g/mol) and it was diluted into a 50:50 (w/w) solution in  $\gamma$ -butyrolactone. Imidazole (Fluka) was used as crosslinking catalyst (0.06 wt % of the solid content of the reaction mixture) in the carboxylic acid reaction with epoxy. Triarylsulfonium hexafluoroantimonate salt solution (50 wt % salt in polypropylene carbonate; Aldrich) was added (2.5 wt % of the epoxy content) as an acid catalyst precursor that decomposed to cations upon exposure to ultraviolet light ( $\lambda = 365$  nm, 17 mW/cm<sup>2</sup> for 30 s) and catalyzed the ring-opening crosslinking reaction of the residual epoxy groups.

### Preparation of network precursors

The oligomeric PCL prepolymers were melt-polymerized from CL at 150°C in a batch reactor under nitrogen atmosphere. The monomer was fed to the preheated reactor with an appropriate amount of the PGL initiator (3.85 or 9.10 mol %) and 0.02-mol % SnOct<sub>2</sub> catalyst. The reaction time was 5 h and the batch sizes were 0.5 kg. The hydroxyl end-functionalities of the prepolymer were converted to carboxylic acid functionalities by reaction with SA for 2 h at 150°C. The prepolymer and an equimolar amount of anhydride in relation to the hydroxyl groups were fed to the reactor. No catalyst was used. Later on in the text the oligomers are denoted as PCLX-Y, with X correspond-

ing to the number of CL units in each branch elongated from the PGL core and Y corresponding to the end-functionality (OH = hydroxyl or SA = carboxylic acid). The reaction schemes for the synthesis and the functionalization with carboxylic acid are shown in Scheme 1.

### Preparation of reactive blending solutions

The PCLX-SA oligomers were mixed into the epoxy solution in 0:100, 5:95, 10:90, 20:80, 30:70, and 40:60 ratios by weight of the solids, i.e. oligomer and epoxy, respectively. The crosslinking catalyst(s) (imidazole and triarylsulfonium hexafluoroantimonate salt solution) were then added. The use of a dual-catalyzed mixture was needed to achieve a high degree of crosslinking because there was an excess of epoxy groups in relation to the carboxylic acid groups of the oligomers. The crosslinking reactions of the dual-catalyzed solution are shown in Scheme 2.

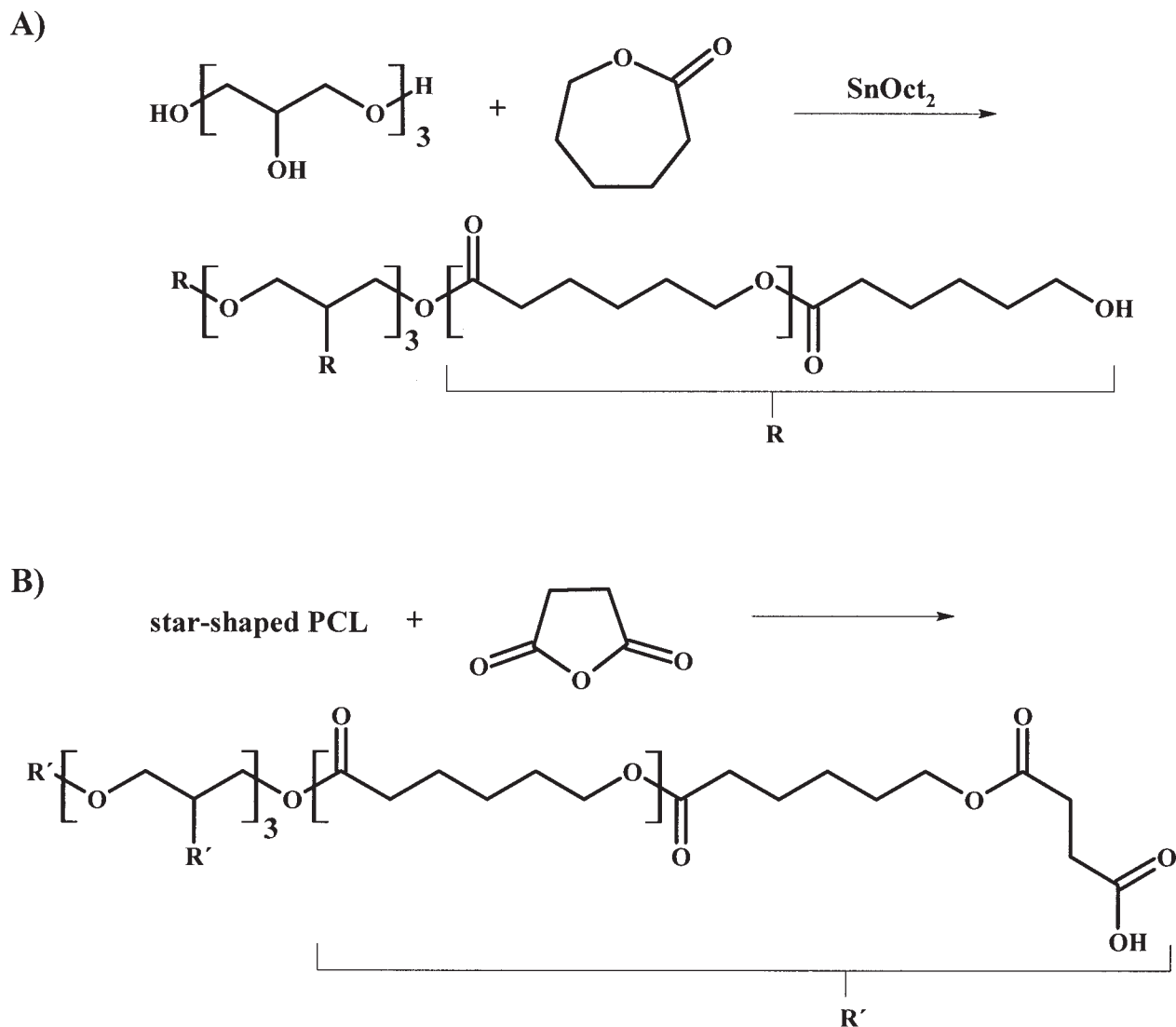
### Coating and crosslinking procedure

A solution of the network precursors (PCLX-SA oligomer and epoxy resin) and the solvent was spin-coated onto a silicon wafer at a speed of 2000 rpm for 30 s. A film thickness of 10–20  $\mu$ m was formed depending on the viscosity of the solution, which was not constant because of the different molecular weights of the oligomers. The solvent was evaporated during the first bake at 90°C for 30 min. Simultaneously, the PCLX-SA reacted with the epoxy groups. After the first bake, the coatings were exposed to ultraviolet light, which released the acid catalyst from the photoinitiator. The cationic ring-opening crosslinking of the residual epoxy groups took place in the second bake at 180°C for 60 min in a convective oven. The preparation of the coatings was carried out in a clean room (class 1000) to avoid surface contamination.

### Characterization

The <sup>1</sup>H NMR spectra were recorded on a Varian XL-300 NMR spectrometer working at 300.032 MHz. The samples were dissolved, at room temperature, in CDCl<sub>3</sub> in 10-mm NMR tubes. The sample concentration was about 1 wt % for proton. Proton decoupled <sup>13</sup>C NMR spectra were obtained with the Varian XL-300 NMR spectrometer working at 75.452 MHz. The sample concentrations in 10-mm tubes were 10 wt % in CDCl<sub>3</sub>.

The number-averaged molecular weight ( $\bar{M}_n$ ), weight-averaged molecular weight ( $\bar{M}_w$ ), and molecular weight distribution (MWD) were determined by size exclusion chromatography (SEC) at room temperature (Waters System Interface module, Waters 510 HPLC Pump, Waters 410 Differential Refractometer,



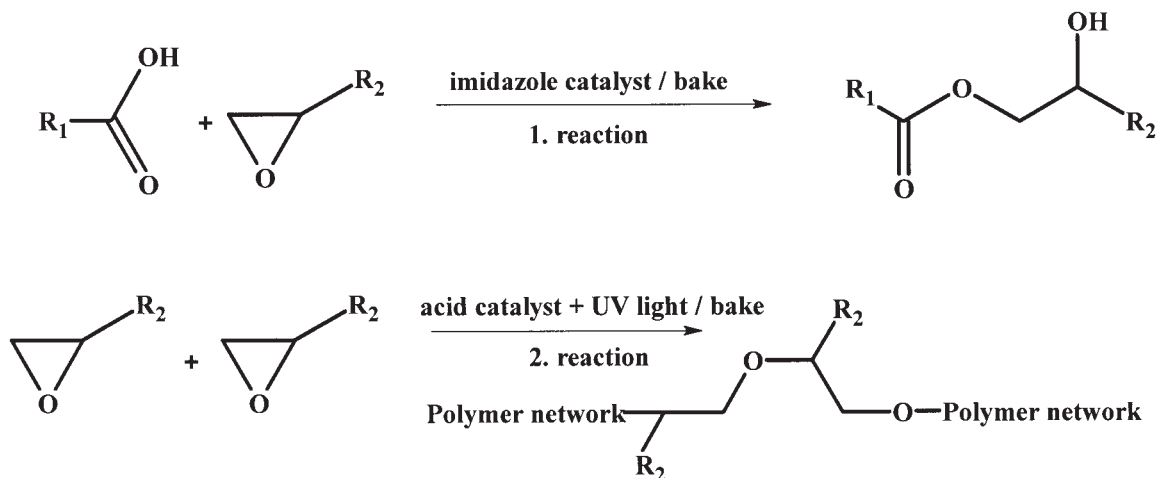
**Scheme 1** Polymerizations of (a) PCLX-OH oligomer and (b) functionalization to PCLX-SA.

Waters 700 Satellite Wisp, and four PL gel columns: 104, 105, 103, and 100 Å connected in series). Mono-disperse polystyrene standards were used for primary calibration. Chloroform (Riedel-de Haën; stabilized with 1% ethanol) was used as solvent and eluent. The injected volume was 200  $\mu\text{L}$  and the flow rate was 1 mL/min.

Differential scanning calorimetric (DSC) measurements were carried out on a Mettler Toledo Star DSC821 in the temperature range  $-100^{\circ}\text{C}$  to  $100^{\circ}\text{C}$  for the oligomers and  $100$ – $210^{\circ}\text{C}$  for the crosslinked samples, at a heating and cooling rate of  $10^{\circ}\text{C}/\text{min}$ . The glass transition ( $T_g$ ) and melting ( $T_m$ ) temperatures of the oligomers were recorded during the second heating period. The residual reactivity and the  $T_g$  of the crosslinked samples were observed from the first heating scan, during which the epoxy groups are expected to reach complete conversion.

Dynamic mechanical analysis (DMA) was performed on a Perkin-Elmer 7 Series instrument. Samples of size  $2 \times 10 \times \sim 0.5 \text{ mm}^3$  were investigated in flexural mode (three-point bending) under a temperature ramp of  $4^{\circ}\text{C}/\text{min}$  at a fixed frequency of 1 Hz. The measurements were carried out over a temperature range of  $-50^{\circ}\text{C}$  to  $250^{\circ}\text{C}$ .

Scanning electron microscopy (SEM) examinations of the cross sections of fractured polymer coatings were carried out to obtain information about the fracture mechanism of the reactively blended epoxy films and to observe morphology. An initial crack was prepared with a diamond pen on the back of a sample, i.e., on the silicon wafer, after which a sharp bending force was applied manually to break the sample. The specimens were sputter-deposited with chromium, with an EmiTech turbo sputter-coater K575-X. All the specimens were examined with a Jeol field emission



**Scheme 2** Reactions of the dual-catalyzed crosslinking of PCLX-SA and epoxy.

scanning electron microscope (JSM-6335F) operated at 5 kV.

The contact angles of sessile drops of distilled water, diiodomethane, and formamide on the coating surfaces were measured with an Advanced Surface Technology goniometer equipped with a VCA 2500XE video contact angle system. For each sample, the contact angle value is the average of eight measurements recorded from different locations on the sample with a standard deviation of 1–3°. Surface free energy ( $\gamma_s$ ) of the solid surface was calculated from the contact angles, using a geometric mean model.<sup>40,41</sup> The geometric mean model was selected from models found in the literature<sup>40–46</sup> on the basis of our earlier evaluation of the various models<sup>19</sup> and the ongoing debate about models.<sup>47–50</sup> The volume of the liquid drop was 0.1  $\mu\text{L}$ . The surface free energy ( $\gamma_s$ ) in the model is assumed to be the sum of dispersion ( $\gamma_s^d$ ) and polar ( $\gamma_s^p$ ) components. The dispersive (d) and polar (p) components for the surface tensions ( $\gamma_{LV}$ ) of the probing liquids adopted here are  $\gamma_{LV} = 72.8 \text{ mJ/m}^2$ ,  $\gamma_{LV}^d = 21.8 \text{ mJ/m}^2$ ,  $\gamma_{LV}^p = 51.0 \text{ mJ/m}^2$  for distilled water;  $\gamma_{LV} = 50.8 \text{ mJ/m}^2$ ,  $\gamma_{LV}^d = 48.5 \text{ mJ/m}^2$ ,  $\gamma_{LV}^p = 2.3 \text{ mJ/m}^2$  for diiodomethane; and  $\gamma_{LV} = 58.2 \text{ mJ/m}^2$ ,  $\gamma_{LV}^d = 39.5 \text{ mJ/m}^2$ ,  $\gamma_{LV}^p = 18.7 \text{ mJ/m}^2$  for formamide.<sup>51</sup>

Human pulmonary artery endothelial cells (HPAE) were obtained from PromoCell (Heidelberg, Germany) and were cultured from passage 4 to passages 13–14 in defined endothelial cell growth medium-2 (PromoCell). The cells were then split once a week using 0.1% trypsin. Trypsin was inhibited by trypsin-neutralizing solution (TNS, PromoCell). For the experiment, the cells were seeded on pristine surface and on surfaces treated with fetal calf serum (FCS) and were fixed after both 4- and 24-h cultures.

Fixations were carried out with 0.1M sodium cacodylate buffered 2.5% (w/v) glutaraldehyde (pH 7.2, EM-grade) for 1 h at +4°C. After fixation the samples

were washed three times with the same buffer. After dehydration in the series of solutions with increasing amount of ethanol in water and finally twice in 100% ethanol, hexamethyldisilazane (HMDS) was used to preserve the original morphology of the cells.<sup>52,53</sup> The samples were mounted on aluminum stubs with silver glue. Chromium was used as coating metal and the sputter coating was done in an EmiTech turbo sputter coater K575-X. All specimens were examined under a Jeol field emission scanning electron microscope JSM-6335F at 5 or 15 kV.

## RESULTS AND DISCUSSION

The synthesis of crosslinkable PCL consisted of two steps (Scheme 1). First, CL-based star-shaped oligomers were polymerized. In the second step, the hydroxyl groups of the oligomers were converted to carboxylic acid end-functionalities by reaction with SA. Reactive blends were prepared from the carboxylic acid functionalized oligomers and epoxy, and thin polymer films were laid on silicon substrates by spin coating. Finally, the films were crosslinked with the use of the dual catalyst (Scheme 2). In the following subsections, we report the synthesis of the functionalized oligomers, the reactive blending, and selected surface and bulk characteristics of the crosslinked polymer blends.

### Polymerization of hydroxyl end-functionalized oligomers

The use of multihydroxyl-functionalized PGL initiator in ring-opening polymerization (ROP) of CL enables the preparation of star-shaped oligomers.<sup>36</sup> The molecular weight of the oligomer varied with the ratio of PGL to CL in the feed (Table I). Since the amount of the  $\text{SnOct}_2$  catalyst was very low in relation to the OH

TABLE I  
Properties of the PCLX-OH and End-functionalized PCLX-SA Oligomers

Oligomer <sup>a</sup>	DSC		SEC			Theoretical <sup>b</sup> $\bar{M}_n^c$ (g/mol)
	$T_g$ (°C)	$T_m$ (°C)	$\bar{M}_w$ (g/mol)	$\bar{M}_n$ (g/mol)	MWD	
PGL	-42	n.d. <sup>c</sup>	n.d.	n.d.	240	
PCL2-OH	-59	6,19	2780	2220	1.3	1360
PCL5-OH	-60	33,40	6260	5290	1.2	3040
PGL-SA	1	-	n.d.	n.d.	n.d.	740
PCL2-SA	-41	-	6250	4110	1.5	1860
PCL5-SA	-44	30,37	20300	8060	2.5	3540

<sup>a</sup> The number refers to the theoretical amount of CL units per arm; SA, succinic anhydride.

<sup>b</sup> Calculated as  $[\text{CL}]/[\text{PGL}] \times M(\text{CL}) + M(\text{PGL}) + 5 \times M(\text{SA})$ .

<sup>c</sup> n.d., not determined because of insolubility in the eluent.

groups in the PGL initiator ( $[\text{SnOct}_2]/[\text{OH}] = \sim 0.001\text{--}0.002$ ), the  $\text{SnOct}_2$  must have acted as a catalyst rather than as an initiator in this ROP, which follows a coordination–insertion mechanism as has been pointed out by Dong et al.,<sup>54</sup> using comparable reaction conditions. The role of  $\text{SnOct}_2$  as a catalyst is in agreement with the general understanding that alteration of the PGL/CL ratio can be used to tailor the molecular weight of the oligomers.  $^1\text{H}$  NMR study showed the conversion of the CL to be close to 100%, because there was no peak for the CL monomer ( $-\text{CH}_2-\text{COO}-$ ) at 2.63 ppm. The average number of CL units in each arm can be determined by end-group analysis, which can be adequately done for oligomers by NMR. It is to be noted that, for a multiarm structure, end-group analysis yields average arm length and not absolute length. From the low concentration of  $\text{SnOct}_2$ , we assume that the arms start to grow one after the other as the catalyst becomes available for the PGL hydroxyl groups. The growing branches probably create steric hindrance over some of the initiator's hydroxyl groups, which in turn decreases the branching below the amount expected on the basis of the structure of the initiator. In addition, on the basis of the roles of catalyst and initiator noted above, it is likely that the arms are of different length. This being the case, the end-group analysis yields only an average degree of branching and an average chain length of the branches.

The number of arms of the star-shaped oligomers was determined by  $^{13}\text{C}$  NMR analysis. Although the  $^1\text{H}$  NMR spectra are more sensitive, they cannot be used for quantitative analysis because some peaks of the PGL initiator overlapped the region of interest. By way of example, the  $^{13}\text{C}$  NMR spectrum of the PCL5-OH oligomer is shown in Figure 1(a). For this oligomer, the average number of CL units per arm was calculated to be 6.1. The calculation was based on the integrated resonances at 173.5 and 173.3 ppm, assigned to carbons "6" and "12" respectively, in Figure 1(a). It was expected that if all five hydroxyl groups of the PGL initiate the polymerization reaction

of CL the number of CL units per arm would be 5.0. Thus, the measured and predicted number of CL units per arm did not match. The number of the CL units (96.15 mol %) per PGL unit (3.85 mol %) in the feed was 25, which suggests the presence of four arms ( $25/6.1 = 4.1$ ), on average, for the oligomer. In summary, only four hydroxyl groups of the five available in the initiator were capable of initiating the ROP reaction. This is in agreement with earlier studies carried out with eight functional initiator and CL (6/8 OH groups reacted)<sup>35,36</sup> and with six functional initiator and lactide (4/6 OH groups reacted).<sup>55</sup>

DSC analysis of the star-shaped PCL oligomers was carried out to obtain information about their structure. The PGL initiator was amorphous, but the incorporation of CL arms resulted in a semicrystalline structure (Table I). Oligomers PCL2-OH and PCL5-OH both exhibited two melting endotherms. Multiple melting endotherms are generally observed for branched polymers,<sup>56–58</sup> although the reason for this is not clear. We propose that the star-shaped oligomers exhibit arms of different length, each with a different ability to form crystalline domains during solidification. As discussed earlier, the formation of arms of different length is likely for star-shaped oligomers prepared in the presence of low concentration of  $\text{SnOct}_2$ . Previously,<sup>36</sup> it was shown that as the proportion of CL increases, i.e., the molecular weight increases, the thermal properties of star-shaped oligomers approach those reported<sup>59</sup> for linear high-molecular-weight PCL ( $T_g = -60^\circ\text{C}$ ,  $T_m = 60^\circ\text{C}$ ). This tendency was observed here too and the thermal properties of the four-armed oligomers were similar to those reported<sup>36</sup> for the six-armed oligomers of comparable molecular weight.

SEC was used to follow the influence of the PGL/CL ratio on molecular weight. As expected, the molecular weight could be tailored with the amount of PGL (Table I). The ROP of CL yielded oligomers with controlled structure and with narrow MWD in the range of 1.2–1.3. We note, however, that the SEC instrument was calibrated with narrow polystyrene standards, so that the SEC results were affected not

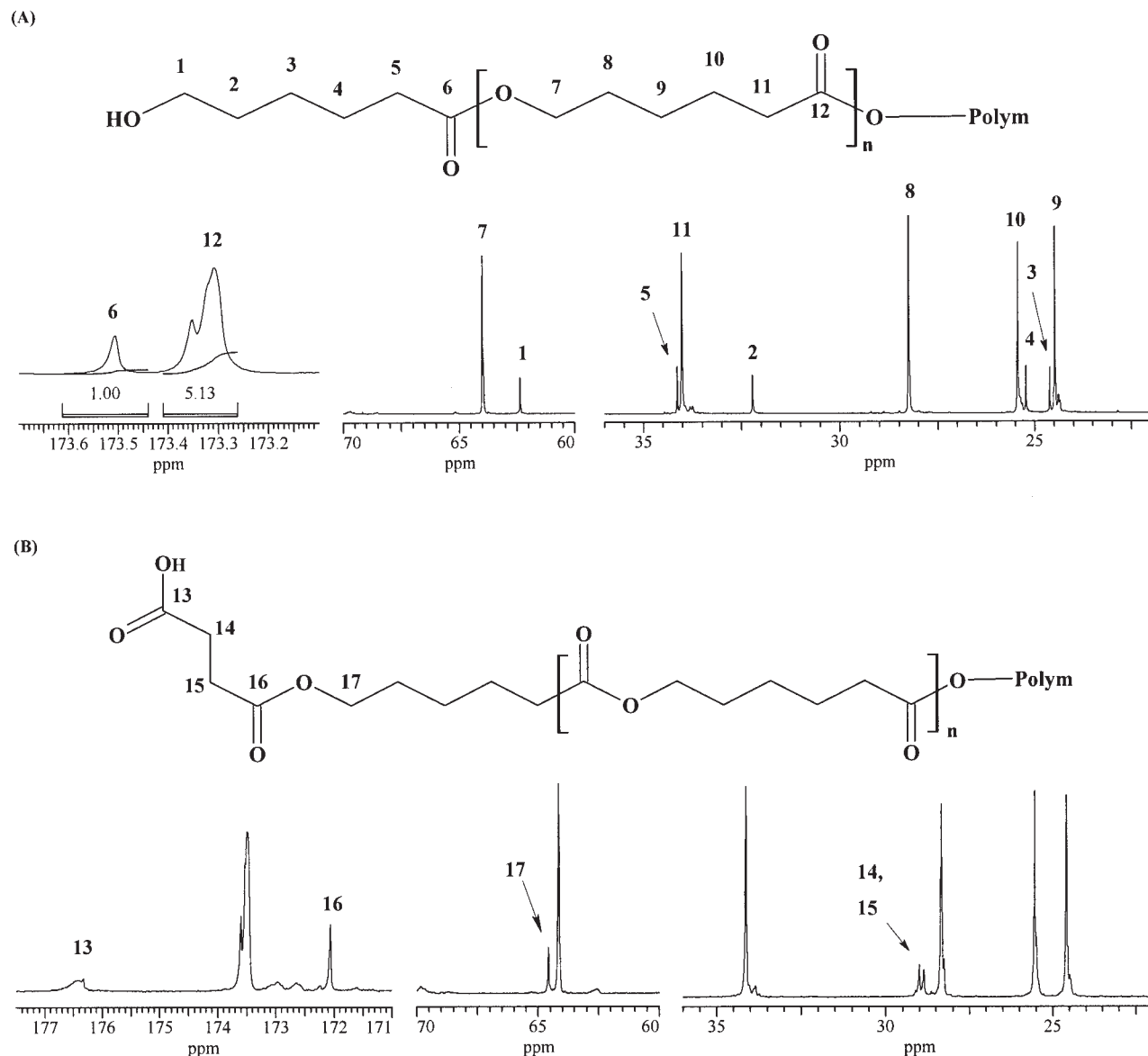


**Figure 1**  $^{13}\text{C}$  NMR spectra of (a) PCL5-OH and (b) end-functionalized PCL5-SA oligomers.

only by the size of the molecule but also by the structure. The values obtained by SEC thus differed slightly from the theoretical  $\bar{M}_n$  values. A trend of decreased  $\bar{M}_n$  with increased amount of PGL could nevertheless be seen. In addition, the SEC curves of the oligomers were symmetrical and unimodal, and no traces of unreacted CL were detected. Hence, the tailoring of the oligomer structure was controlled and the conversion was high according to both NMR and SEC analyses.

Molecular weight analysis of highly branched polymers is difficult and few methods give "absolute" values. In the case of highly controllable polymerizations such as ROP, the measured value should coincide with the theoretical  $\bar{M}_n$ . It is reported<sup>60</sup> that SEC gives a higher  $\bar{M}_n$  value than multiangle laser light

scattering (MALLS), which is considered to be an accurate method resulting in "absolute" value for  $\bar{M}_n$ . In addition, SEC analysis of linear polymers result in higher molecular weight value than the analysis of branched polymer with similar molecular weight. This is because branched polymers assume a more tightly packed structure than their linear counterparts, which are used in the calibration of SEC and assume a random coil structure. The  $\bar{M}_n$  value for the four-armed oligomers that we obtained by SEC was higher than the theoretical  $\bar{M}_n$  calculated from the feed ratio. We attribute this to the significant difference in the hydrophilicity of the core molecule and the CL arms, which causes the oligomers (PCLX-OH) to assume a spatially star-shaped rather than a tightly packed structure in the SEC analysis.

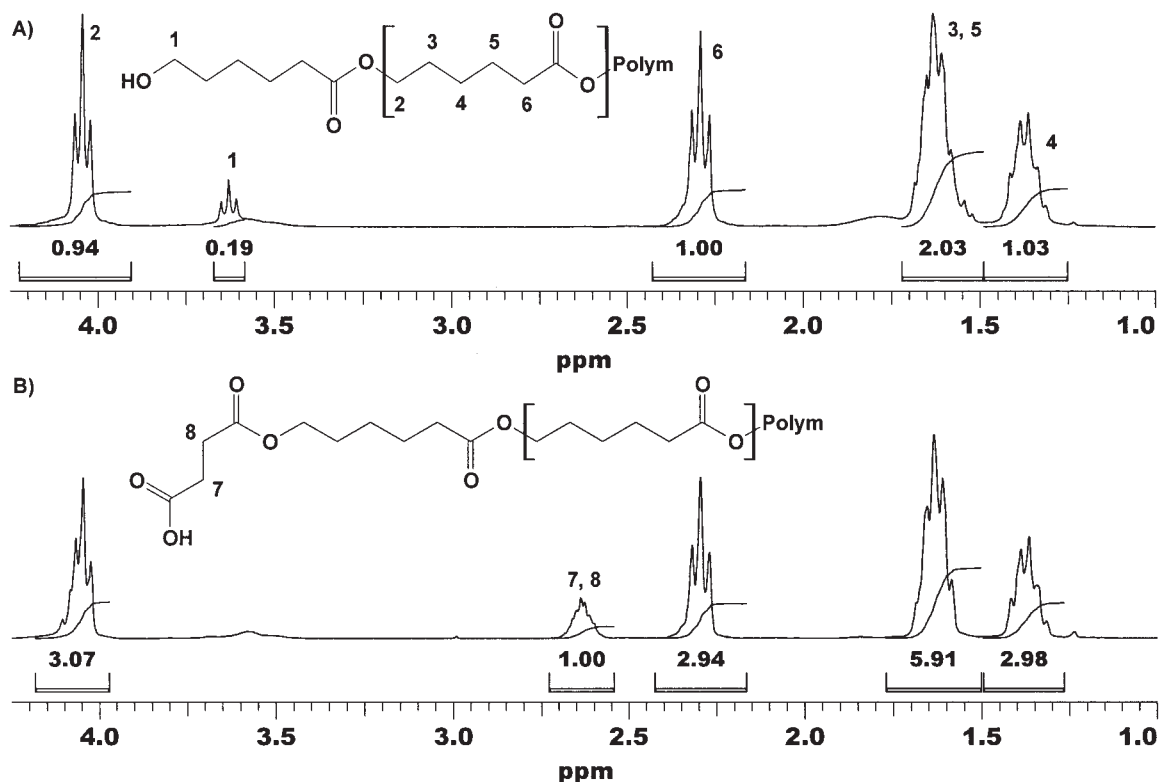


Figure 2  $^1\text{H}$  NMR spectra of (a) PCL5-OH and (b) end-functionalized PCL5-SA oligomers.

### Carboxylic acid functionalization

The oligomers' hydroxyl end-groups were converted to carboxylic acid groups by reaction with SA. The degree of functionalization was high according to NMR analysis [cf. Figs. 1(a) and 1(b)]. The peaks in the  $^{13}\text{C}$  NMR spectrum for the end-group carbons of the oligomer ( $\text{CH}_2\text{—CH}_2\text{—OH}$ ) assigned as "1" and "2" in Figure 1a disappeared as a result of the functionalization. The exchange of the terminal groups was verified by  $^1\text{H}$  NMR analysis. The carboxylic acid group caused a peak at 2.64 ppm, which originated from the protons attached to the two carbon atoms in the new end-group, assigned as "7" and "8" in Figure 2(b). Measurement of the peak intensity made possible a quantitative analysis of the degree of functionalization. Disappearance of the hydroxyl end-group peak at 3.58 ppm and the value of the end-group/CL ratio (SA/CL) led us to conclude that functionalization of oligomers reacted with SA was complete. The SA/CL ratio was 1/6, in agreement with the  $^{13}\text{C}$  NMR results. The detailed chemical structure characterization of the functionalized oligomer, based on the  $^1\text{H}/^{13}\text{C}$  NMR analyses, is shown in Figures 1(b) and 2(b). The glass transition temperature increased with the carboxylic acid functionalization probably owing to the increase in intermolecular hydrogen bonding. The amorphous nature of the PCL2 oligomer increased after the functionalization and the melting endotherms disappeared

(Table I). PCL5 oligomer, however, which had longer CL segments, continued to exhibit double melting endotherms.

### Reactive blending of epoxy with end-functionalized oligomer

We anticipated that the synthesized four-armed oligomer could be used to effectively toughen the inherently brittle SU8 epoxy. In addition, we expected that the use of a flexible core molecule, PGL, as initiator rather than pentaerythritol, which has previously been used as an initiator for polylactide polymerization,<sup>61</sup> would enhance the plasticization effect. The end-functionalization enabled reaction between the oligomer and the epoxy resin, which has been reported to reduce the phase separation while giving rise to toughening.<sup>33,34</sup> Reaction-induced phase separation may, however, still occur during the crosslinking of a two-component reaction mixture because the solubility of the components decreases as a function of the increasing molecular weight of the network.<sup>25,62,63</sup>

DSC provided first-hand information about the crosslinked networks. According to the DSC analyses, the crosslinked epoxy exhibited a  $T_g$  around 180°C, and as expected, the  $T_g$  of the reactively blended epoxies was slightly lower than that. A high  $T_g$  is considered beneficial for many applications in electronics.

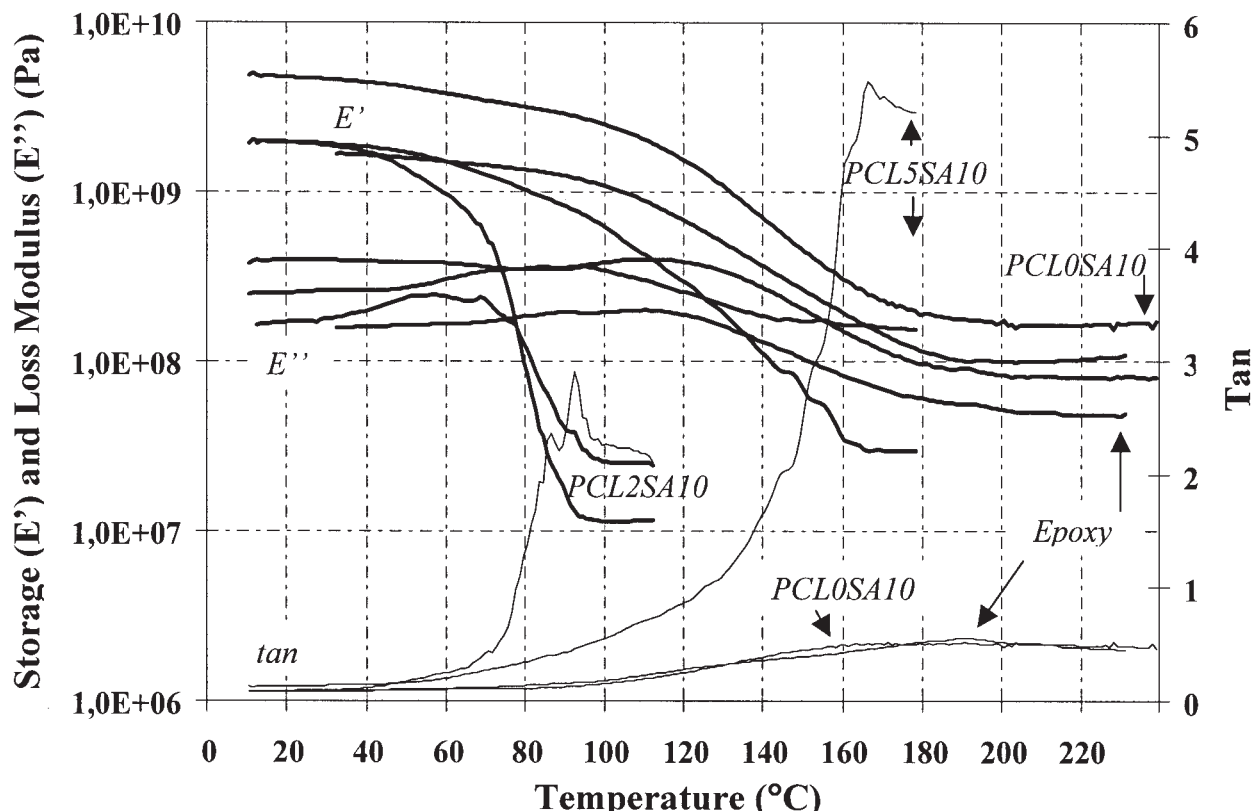


**Figure 3** Storage ( $E'$ ) and loss modulus ( $E''$ ) and  $\tan \delta$  of the crosslinked epoxy and its crosslinked blends prepared with 10 wt % of PCL0-SA, PCL2-SA, and PCL5-SA.

Both the size of the macromolecule and the proportion of the oligomer affected the  $T_g$ . Some of the samples exhibited two  $T_g$ 's, indicating inadequate incorporation of PCLX-SA into the network. However, the second  $T_g$  was weak and broad, which means that the degree of PCLX-SA incorporation into the network must have been considerable. Also the primary  $T_g$  appeared as a weak peak. DMA was accordingly employed to obtain more information about the network structure.

### Thermomechanical properties

DMA has been used to detect two-phase structures in polymer blends, providing at the same time thermo-mechanical information.<sup>64</sup> Here, we investigated the network structure of the crosslinked epoxy and the effect of the type and amount of the oligomer on the thermomechanical properties of the reactively blended epoxies.

The dynamic mechanical properties of the four epoxies are shown in Figure 3, and the glass transition temperatures determined from the  $\tan \delta$  curves are given in Table II. In a comparison of blends with 10 wt % concentration of the oligomer, the PCL0-SA modifier with smallest molecular weight provided the highest  $T_g$ . In addition, the elastic modulus at the glassy

state was significantly higher with PCL0-SA than with other oligomers and the epoxy. This is attributed to the denser crosslinking enabled with the smallest PCL0-SA oligomer. The crosslinking densities were evaluated from the storage modulus at the rubbery plateau according to the theory of rubber elasticity.<sup>64</sup> The molecular weights between crosslinks ( $\bar{M}_c$ ) are shown in Table II.

For all networks, the storage modulus at glassy state did not decrease from that of the epoxy, but the  $T_g$  decreased, indicating plasticization of the material.

**TABLE II**  
Glass Transition Temperatures for the Selected Network Samples as Determined from Storage Modulus Curves Obtained by DMA

	$T_g$ ( $\tan \delta$ ) (°C)	$E' \ll T_g$		$\bar{M}_c$ (g/mol)
		$T < T_g$	$T > T_g$	
Epoxy	191	$1.7 \times 10^9$	$1.0 \times 10^8$	50
PCLO-SA10	165	$5.0 \times 10^9$	$1.7 \times 10^8$	30
PCL2-SA10	93	$2.0 \times 10^9$	$1.1 \times 10^7$	300
PCL5-SA10	167	$2.0 \times 10^9$	$3.0 \times 10^7$	100
PCL2-SA5	160	$2.5 \times 10^9$	$1.5 \times 10^8$	30
PCL2-SA20	139	$1.3 \times 10^9$	$9.7 \times 10^6$	400
PCL2-SA30	60,91	$5.8 \times 10^9$	$6.0 \times 10^6$	600
PCL2-SA40	94	$3.8 \times 10^9$	$7.0 \times 10^6$	500



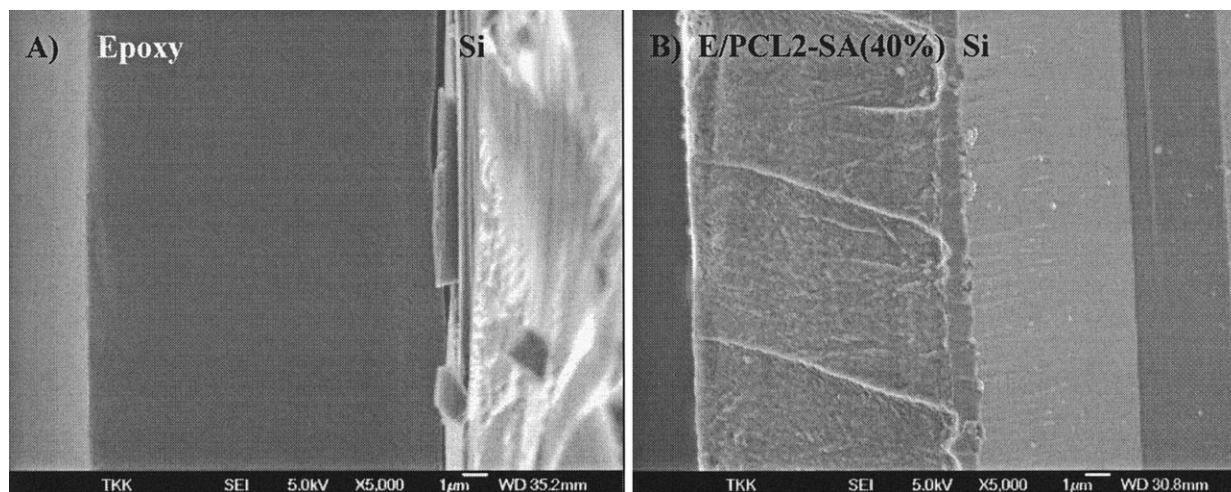


**Figure 4** Comparison of the fractured surfaces of (a) the epoxy and (b) blend film (40 wt % of PCL2-SA in the epoxy).

The middle-sized oligomer (PCL2-SA) plasticized most effectively (with 10 wt % usage). The largest oligomer (PCL5-SA) did not enable high density of crosslinking. Also, because of its smaller molecular proportion in the blends in comparison with PCL0-SA and PCL2-SA (with the fixed 10 wt % blending), the plasticization effect was reduced and therefore the  $T_g$  remained high.

The influence of concentration of the middle-sized oligomer on the thermomechanical properties and the crosslinking density is shown in Table II. With high concentration (40 wt %) of the oligomer the storage modulus of the blend at glassy state was significantly increased but the  $T_g$  decreased clearly. Indirectly, this is an indication of increased flexibility of the material. In practice, this was observable by bending both epoxy and blend-coated samples of a flexible PWB. The epoxy-coated sample showed cracking whereas the blend-coated samples were crack-resistant. In addition, a comparison of the loss modulus curves showed that significantly more energy is dissipated in deformation of the PCL2-SA modified blend than in deformation of the brittle homogeneous epoxy. The brittle fracture that occurs when the epoxy film is broken changes to a more ductile for the blend with 40 wt % of PCL2-SA as shown in Figure 4.

Depending on the crosslinking parameters (time and temperature) and molar concentrations, a network structure ranges from a homogeneous network to a phase-separated blend. Phase-separation, however, was not investigated in this study. The two-phased structure, resulting from the inadequate reaction between the oligomer and the epoxy before the second reaction step commenced, could be revealed by DMA. However, the thermomechanical transitions of the blends were too broad for drawing meaningful conclusions about reaction-induced phase separation. The broadness of the transitions is a common problem

with highly crosslinked polymers.<sup>65</sup> However, the reaction mixture was transparent initially, which indicated that the components were soluble in each other. The prebaked coatings were still transparent, which means that the oligomers and the precrosslinked network must have been soluble in the epoxy. The use of PCL0-SA and PCL2-SA oligomers in high concentration (40 wt %) resulted in a hazy appearance after the second step of crosslinking, indicating severe phase separation.

#### Surface free energy–contact angle measurements

The properties of surfaces are of key importance in the manufacturing of bioadaptive devices. The SU8 epoxy has good material and processing properties and it has been used to prepare, e.g.,  $\mu$ -fluidic channels<sup>66</sup> that can be utilized in miniaturized biomedical devices like lab-on-a-chips. After the modification, the use of the epoxy in the fabrication of flexible integrated module boards (IMBs),<sup>18</sup> in particular, would be possible. Because there are many emerging applications in the field of bioengineering, the study of the surface properties and biocompatibility of the modified epoxies is essential.

With this end in view, one of the objective of the present study was to determine the effect of the reactive blending on endothelial cell spreading. The degree of hydrophilicity of the surface has a particular influence on biocompatibility and cell spreading, therefore, the surface energetics has to be investigated first.

The surface free energies and the hydrophobic ( $\gamma_{sv}^d$ ) and hydrophilic ( $\gamma_{sv}^p$ ) components were calculated from the contact angles by the geometric mean model.<sup>40,41</sup> The division into the above-mentioned components allows a discussion of the hydrophilicity/hydrophobicity evolution of the surface. The deter-

**TABLE III**  
**Contact Angles of Deionized Water, Formamide, and Diiodomethane on the Crosslinked Coatings and the Calculated Surface Free Energies**

Crosslinked polymer system	Water (°)	FA (°)	DIM (°)	$\gamma_{sv}$ (mJ/m <sup>2</sup> )	$\gamma_{sv}^p$ (mJ/m <sup>2</sup> )	$\gamma_{sv}^d$ (mJ/m <sup>2</sup> )
Epoxy (E)	80.4	72.2	38.6	41.6	3.7	37.9
E (95 wt %)/PCL2-SA (5 wt %)	83.0	69.2	32.6	43.2	2.4	40.8
E (90 wt %)/PCL2-SA (10 wt %)	86.2	59.2	28.7	44.8	1.2	43.6
E (80 wt %)/PCL2-SA (20 wt %)	79.0	55.3	41.1	39.8	4.8	35.0
E (70 wt %)/PCL2-SA (30 wt %)	93.3	61.5	38.5	40.9	0.4	40.5
E (60 wt %)/PCL2-SA (40 wt %)	76.1	67.6	36.7	42.3	5.6	36.7
E (90 wt %)/PCLO-SA (10 wt %)	85.8	71.1	40.8	39.2	2.2	37.0
E (90 wt %)/PCL5-SA (10 wt %)	85.5	63.5	35.7	41.7	1.9	39.8

mined surface free energies are shown in Table III. All the coatings were fairly hydrophobic. The blend with 30 wt % PCL2-SA was the most hydrophobic with polarity ( $X_p = \gamma_{sv}^p / \gamma_{sv}$ ) of only 1%. The coatings with 20 and 40 wt % of the PCL2-SA had lower contact angles with water than with the other coatings, indicating more hydrophilicity.

The contact angle with water for a linear PCL diol oligomer made up of 11 CL units is about 40° and it increases with the number of CL units.<sup>67</sup> The four-armed PCL2-SA oligomer has 10 CL units and could be expected to exhibit similar or perhaps slightly smaller contact angle with water than that reported for the PCL diol, since it has a relatively large hydrophilic core (the PGL initiator) and carboxylic acid end-groups capable of forming hydrogen bonds. Assuming that the contact angle between water and the end-functionalized oligomer is roughly half that for the cured epoxy (80.4°), we expected that the contact angle for the epoxy would decrease with incorporation of the oligomer, resulting in increased hydrophilic character. However, the crosslinking reactions affect the chemistry of the incorporated network precursors,<sup>19</sup> and the final surface properties were not simply a sum of the surface properties of the incorporated molecules.

During the first step of the dual-catalyzed crosslinking, equimolar amounts of epoxy groups in relation to acid groups were reformed to ester links between the oligomer and epoxy resin molecules. During the second step of the crosslinking the residual epoxy groups were reformed to ether links between the epoxy resin molecules. Furthermore, the hydrophilic functional groups will be directed toward the bulk material instead of the material/air interface if this is kinetically possible, because the system strives to minimize its total free energy. Several groups<sup>12,67,68</sup> have noticed that the hydrophilic groups tend to redirect into the bulk, though they were intentionally created on the surface. The water contact angles were higher on blend surfaces than on epoxy surfaces and it is expected that, also here, the hydrophilic groups were directed towards the bulk.

### Cell culture

The evaluated surfaces were made as smooth as possible by the spin coating method to minimize the influence of topography on the cell response. The average roughness of the epoxy film was earlier measured to be 0.3 nm,<sup>19</sup> so, the effect of topography on the cell spreading can be considered minor.

The cells grown on pristine surfaces were flat showing good affinity to the reference epoxy (SU8) as well as to most of the blend surfaces. Pretreatment with FCS enhanced cell adhesion to the reference. Response was poor with the highly hydrophobic coatings and the cells appeared round emitting significantly more filopodia than those on slightly modified surfaces.

Spreading of endothelial cells on synthetic surfaces is difficult. We achieved almost 40% coverage with FCS-pretreated epoxy and a pristine blend containing 20 wt % PCL2-SA, which is considered to be fairly high coverage for a 24-h culture. Others have reported coverage between 10% and 20% on flat polybromostyrene-polystyrene and poly-*n*-butylmethacrylate-polystyrene systems and more on roughened surfaces.<sup>69,70</sup> Our preliminary tests of the biocompatibility of the modified epoxy coatings indicate, therefore, that the endothelial cells tolerated the evaluated materials well. Additional biocompatibility testing will be required to gain a better understanding of behavior in the vicinity of living tissue if implantation of such materials is to be considered.

### CONCLUSIONS

Four-armed CL-based oligomers were synthesized and end-functionalized with SA to enable reactive blending with the epoxy resin. The ROP of CL in the presence of PGL initiator (3.9 and 9.1 mol %) and SnOct<sub>2</sub> catalyst yielded oligomers with hydroxyl end-groups, which were completely converted to carboxylic acid groups during the functionalization stage. Thorough characterization of the oligomers showed that their structure could be tailored in a controlled manner by changing the ratio of initiator to mono-

mer(s) in the feed. A high degree of crosslinking is required for effective modification of the epoxy with the oligomer. To achieve an adequately crosslinked network, a dual-catalyzed reaction scheme was employed in which the oligomer was first incorporated into the epoxy matrix in the imidazole-catalyzed reaction. A second step was used to complete the crosslinking and this was carried out in the acid-catalyzed ROP of the residual epoxies. Application of the PCL2-SA oligomer to the epoxy resulted in a noticeable increase in toughness according to combined microscopy and thermal investigations, while the  $T_g$  was decreased only slightly. The blending increased surface hydrophobicity and did not affect significantly the inherently advantageous spreading of endothelial cells. The results showed that the use of toughened SU8 with flexible PWBs is possible, and that modification of the surface properties makes the use in devices converging on biointerfaces a feasible option.

The authors express their gratitude to Dr. Kari Lounatmaa for the help in the cell fixation and SEM investigation and Prof. M.D. Ismo Virtanen for the cell cultures.

## References

- Brown, W. D. *Advanced Electronic Packaging: With Emphasis on Multichip Modules*; IEEE Press: Piscataway, 1999.
- Kricka, L. J. *Clin Chim Acta* 2001, 307, 219.
- Griese, E. *IEEE Trans Adv Packag* 2001, 24, 375.
- Lee, K. Y.; LaBianca, N.; Rishon, S. A.; Zolgharnain, S.; Gerlome, J. D.; Shaw, J.; Chang, T. H. P. *J Vac Sci Technol B* 1995, 3012.
- Lorenz, H.; Despont, M.; Fahrni, N.; Brugger, J.; Vettiger, P.; Renaud, P. *Sensor Actuat A: Phys* 1998, 64, 33.
- Becker, H.; Locascio, L. E. *Talanta* 2002, 56, 267.
- Genolet, G.; Despont, M.; Vettiger, P.; Anselmetti, D.; de Rooij, N. F. *J Vac Sci Technol B* 2000, 18, 617.
- Weigl, B. H.; Bardell, L. D.; Cabrera, C. R. *Adv Drug Deliv Rev* 2003, 55, 349.
- Krawczyk, S. *Phys Stat Sol C* 2003, 3, 998.
- Immonen, M.; Karppinen, M.; Kivilahti, J. K. Fabrication and characterization of optical waveguides embedded on printed wiring boards; 3rd International IEEE Conference on Polymers and Adhesives in Microelectronics and Photonics, Montreux, Switzerland, 21–23 Oct 2003.
- Turunen, M. P. K.; Immonen, M.; Kivilahti, J. K. Evaluation of the environmental reliability of polymer waveguides fabricated on printed wiring board; 3rd International IEEE Conference on Polymers and Adhesives in Microelectronics and Photonics, Montreux, Switzerland, 21–23 Oct 2003.
- Ge, J.; Kivilahti, J. K. *J Appl Phys* 2002, 92, 3007.
- Turunen, M. P. K.; Laurila, T.; Kivilahti, J. K. *J Polym Sci Part B: Polym Phys* 2002, 40, 2137.
- Turunen, M. P. K.; Marjamäki, P.; Paajanen, M.; Lahtinen, J.; Kivilahti, J. K. *Microelectron Reliab* 2004, 44, 993.
- Siau, S.; Vervaet, A.; Schacht, E.; van Calster, A. J. *Electrochem Soc* 2004, 151, C133.
- Ge, J.; Turunen, M. P. K.; Kivilahti, J. K. *Thin Solid Films* 2003, 440, 198.
- Ge, J.; Turunen, M. P. K.; Kusevic, M.; Kivilahti, J. K. *J Mater Res* 2003, 18, 2697.
- Ge, J.; Turunen, M. P. K.; Kivilahti, J. K. *J Polym Sci Pol Phys* 2003, 41, 623.
- Romig, A. D., Jr.; Dugger, M. T.; McWhorter, P. J. *Acta Mater* 2003, 51, 5837.
- Lee, M.-W.; Jo, S.-B.; Lee, K.-C.; Kim, K.-W.; Park, S.-G.; Lee, S.-G.; Lee, E.-H.; Beom-Hoan, O. *Thin Solid Films* 2004, 447, 615.
- Meyer, J.-U.; Stieglitz, T.; Scholz, O.; Haberer, W.; Beutel, H. *IEEE Trans Adv Packag* 2001, 24, 366.
- Kujala, A.; Tuominen, R.; Kivilahti, J. K. Solderless interconnection and packaging technique for embedded active components; 49th Electronic Component Technology Conference, San Diego, USA, 1–4 June 1999.
- Feng, R.; Farris, R. J. *J Mater Sci* 2002, 37, 4793.
- Palm, P.; Määttänen, J.; De Maquill, Y.; Picault, A.; Vanfleteren, J.; Vandecasteele, B. *Microelectron Reliab* 2003, 43, 445.
- Kim, B. S.; Chiba, T.; Inoue, T. *Polymer* 1995, 36, 67.
- Bartlet, P.; Pascault, J. P.; Sautereau, H. *J Appl Polym Sci* 1985, 30, 2955.
- Ratna, D. *Polymer* 2001, 42, 4209.
- Okamoto, Y. *Polym Eng Sci* 1983, 23, 222.
- Chen, J.-L.; Chang, F.-C. *Macromolecules* 1999, 32, 5348.
- Bucknall, C. B.; Partridge, I. K. *Polymer* 1983, 24, 639.
- Varley, R. J.; Hodgkin, J. H.; Simon, G. P. *Polymer* 2001, 42, 3847.
- Wu, S. J.; Lin, T. K.; Shyu, S. S. *J Appl Polym Sci* 2000, 75, 26.
- Punchaipetch, P.; Ambrogio, V.; Giamberini, M.; Brostow, W.; Carfagna, C.; D'Souza, N. A. *Polymer* 2002, 43, 839.
- Raghava, R. S. *J Polym Sci Part B: Polym Phys* 1987, 25, 1017.
- Turunen, M. P. K. Master's thesis (in Finnish); Espoo, Finland, 1999.
- Turunen, M. P. K.; Tuominen, J.; Korhonen, H.; Seppälä, J. V. *Polym Int* 2002, 51, 92.
- Boogh, L.; Petterson, B.; Månson, J.-A. E. *Polymer* 1999, 40, 2249.
- Ratna, D.; Simon, G. P. *Polymer* 2001, 42, 8833.
- Turunen, M. P. K.; Laurila, T.; Kivilahti, J. K. *J Appl Polym Sci*, to appear
- Owens, D. K.; Wendt, R. C. *J Appl Polym Sci* 1969, 13, 1741.
- Kaelble, D. H.; Uy, K. C. *J Adhes* 1970, 2, 50.
- Fox, H. W.; Zisman, W. A. J. *J Colloid Sci* 1950, 5, 514.
- Kwok, D. Y.; Neumann, A. W. *Colloids Surf A* 2000, 161, 31.
- Fowkes, F. M. *J Phys Chem* 1963, 67, 2538.
- Wu, S. J. *J Polym Sci Part B: Polym Phys* 1971, 34, 19.
- van Oss, C. J.; Chaudhury, M. K.; Good, R. J. *Chem Rev* 1988, 88, 927.
- Makkonen, L. *Langmuir* 2000, 16, 7669.
- Morrison, I. D. *Langmuir* 1991, 7, 1833.
- Della Volpe, C.; Maniglio, D.; Brugnara, M.; Siboni, S.; Morra, M. *J Colloid Interf Sci* 2004, 271, 434.
- Siboni, S.; Della Volpe, C.; Maniglio, D.; Brugnara, M. *J Colloid Interf Sci* 2004, 271, 454.
- Ma, K.; Chung, T. S.; Good, R. J. *J Polym Sci Pol Phys* 1998, 36, 2327.
- Leikas-Lazányi, P.; Lounatmaa, K. In *Extended Abstracts of the 46th Annual Meeting of the Scandinavian Society for Electron Microscopy (SCANDEM-94)*, Kuopio, Finland, 13–15 June 1994; Tammi, R.; Sorvari, R., Eds.; p 60.
- Nation, J. L. *Stain Technol* 1983, 58, 347.
- Dong, C.-M.; Qiu, K.-Y.; Gu, Z.-W.; Feng, X.-D. *Polymer* 2001, 42, 6891.
- Korhonen, H.; Helminen, A.; Seppälä, J. V. *Polymer* 2001, 42, 7541.
- Tasaka, F.; Miyazaki, H.; Ohya, Y.; Ouchi, T. *Macromolecules* 1999, 32, 6386.
- Li, Y.; Kissel, T. *Polymer* 1998, 39, 4421.
- Arvanitoyannis, I.; Nakayama, A.; Kawasaki, N.; Yamamoto, N. *Polymer* 1995, 36, 2947.
- Hiljanen-Vainio, M.; Karjalainen, T.; Seppälä, J. V. *J Appl Polym Sci* 1996, 59, 1281.
- Minaki, N.; Kanki, K.; Masuda, T. *Polymer* 2003, 44, 2303.

61. Helminen, A.; Korhonen, H.; Seppälä, J. V. *J Appl Polym Sci* 2002, 86, 3616.
62. Ishii, Y.; Ryan, A. J.; Clarke, N. *Polymer* 2003, 44, 3641.
63. Chen, J.-L.; Chang, F.-C. *Polymer* 2001, 42, 2193.
64. Menard, K. P. *Dynamic Mechanical Analysis: A Practical Introduction*; CRC Press: Boca Raton, FL, 1999.
65. Nabeth, B.; Gerard, J. F.; Pascault, J. P. *J Appl Polym Sci* 1996, 60, 2113.
66. Tuomikoski, S.; Franssila, S. *Sensor Actuat A: Phys* 2005, 120, 408.
67. Toselli, M.; Messori, M.; Bongiovanni, R.; Malucelli, G.; Priola, A.; Pilati, F.; Tonelli, C. *Polymer* 2001, 42, 1771.
68. Mayers, D. *Surfaces, Interfaces, and Colloids*; VCH Publishers: New York, 1991.
69. Lin, H. B.; Garcia-Echeverria, C.; Asakura, S.; Sun, W.; Mosher, D. F.; Cooper, S. L. *Biomaterials* 1992, 13, 905.
70. Buttiglieri, S.; Pasqui, D.; Migliori, M.; Johnstone, H.; Affrossman, S.; Sereni, L.; Wratten, M. L.; Barbucci, R.; Tetta, C.; Camussi, G. *Biomaterials* 2003, 24, 2731.